Available online at www.sciencedirect.com
ScienceDirect
Scripta Materialia 60 (2009) 1137–1140
Scripta MATERIALIA
www.elsevier.com/locate/scriptamat

Nanoscale amorphization of severely deformed NiTi shape memory alloys

M. Peterlechner,* T. Waitz and H.P. Karnthaler

Physics of Nanostructured Materials, Faculty of Physics, University of Vienna, Boltzmanngasse 5, 1090 Vienna, Austria

Received 26 January 2009; revised 27 February 2009; accepted 28 February 2009
Available online 6 March 2009

NiTi shape memory alloys deformed by high-pressure torsion (HPT) were investigated by transmission electron microscopy. Radial sections of the HPT discs facilitate the analysis of nanoscale amorphous and crystalline phases. Ultrathin amorphous ribbons forming at grain boundaries are intersected by shear bands. At higher deformation they transform into thicker amorphous bands containing nanocrystalline debris. In the case of planar sections, the presence of amorphous phase can be obscured by overlapping nanocrystals leading to moiré contrast.

Keywords: Amorphization; High-pressure torsion (HPT); Transmission electron microscopy (TEM); NiTi; Shape memory alloys (SMA)

Nanostructured materials are characterized by structural features that are smaller than 100 nm at least in one dimension; these materials can have unique physical properties not obtainable in their coarse-grained counterparts [1]. In bulk materials, strong structural refinement is achieved by severe plastic deformation (SPD) methods, such as high-pressure torsion (HPT) [2]. By applying HPT to disc-shaped specimens, ultrahigh shear strains can be obtained. When NiTi shape memory alloys are subjected to HPT, a complex mixture of nanoscale amorphous and crystalline phases is formed [3,4]. Almost complete amorphization can be obtained when the strain value γ exceeds 800. Several models of strain-induced amorphization have been proposed. It was pointed out that amorphization can occur in the core regions of dislocations [5] and by disclinations [6] stored by HPT, or by a plastic instability leading to the formation of shear bands [7]. However, a detailed analysis of amorphous shear bands has not been reported.

Systematic and in-depth studies of SPD-induced nanostructures are required to obtain a thorough understanding of the mechanisms of their formation and of their impact on the physical properties of materials. Transmission electron microscopy (TEM) is one of the most appropriate tools to analyze these nanostructures [8]. Problems of methodology caused by overlapping nanostructures in TEM have to be carefully addressed; strong moiré contrast artifacts can give rise to misinterpretations [9]. Heterogeneous and textured structures induced by SPD require the analysis of different TEM sections chosen with respect to the principal axes of the deformation. In the case of HPT, most TEM investigations are based on planar sections (PS) taken parallel to the plane of the HPT disc [2] (cf. Fig. 1). Only a few TEM investigations have been carried out using other sections, probably due to the experimental difficulties of preparing the corresponding TEM specimens (typically HPT discs have a thickness of <1 mm) [10,11]. Therefore, the aim of the present paper is to investigate the complex nanostructures of HPT NiTi using two different TEM sections. We demonstrate that considerable new insight into the processes of HPT-induced amorphization can be obtained by TEM using a radial section (RS) that is at a right angle to the PS and also includes the shear direction (SD) (cf. Fig. 1).

In this study, a Ni–50.1 at.% Ti alloy was deformed by HPT (12 turns at a pressure of 4 GPa). Using the HPT discs (0.7 mm thick, 8 mm diameter), TEM specimens with a foil normal along the P and R directions were prepared (cf. Fig. 1). Both TEM sections were taken at a distance of 2.8 mm from the center of the HPT disc (corresponding to $\gamma = 300$) and marked to indicate the SD. Lamellar samples were cut out of the HPT discs parallel to the RS; TEM specimens were obtained by mechanical grinding and ion thinning applying rather small grazing angles and low ion energies. In the thickness direction (i.e. along P), areas were studied that corre-

* Corresponding author. Tel.: +43 4277 51312; fax: +43 4277 51316; e-mail: martin.peterlechner@univie.ac.at

1359-6462/$ - see front matter
doi:10.1016/j.scriptamat.2009.02.055

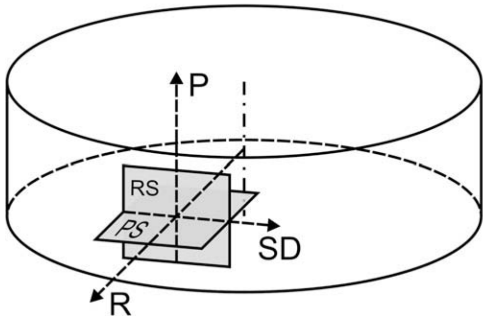

Figure 1. Sketch of a HPT disc. TEM sections denoted as planar section (PS) and radial section (RS) have a foil normal along P and R, respectively. Both PS and RS include the shear direction (SD).

spond to positions near the middle of the HPT disc. In the case of PS, discs with a diameter of 2.3 mm were punched out and used to obtain TEM specimens by electropolishing. Figure 2a and b shows TEM bright-field images of HPT-deformed NiTi corresponding to TEM sections PS and RS, respectively (insets are the selected-area diffraction patterns (SADPs)). The HPT leads to a complex mixture of amorphous and nanocrystalline phases. In both sections amorphous bands are encountered that show a uniform contrast; their traces are almost parallel to the SD (indicated by the double arrow). In the case of PS, the crystalline to amorphous boundaries of the band-shaped areas are frequently curved and rather diffuse. Conversely, in the case of RS, well-defined and straight interfaces are observed. These sharp interfaces agree with an orientation close to edge-on and lead to the conclusion that the amorphous bands are running almost parallel to the PS. The SADPs of both sections show a pattern of diffuse rings caused by the amorphous phase. The diffuse rings are superimposed by diffraction spots of nanograins that have an austenitic (B2) or martensitic (B19′) lattice structure. Using PS, in agreement with previous investigations [8], a rather strong texture $P \| \langle 1\,1\,1 \rangle$ is observed (the B2 lattice is taken as a reference frame). In the case of the RS, texture components are $\langle 1\,\bar{1}\,0 \rangle$ and $\langle 1\,1\,\bar{2} \rangle$ parallel to R and SD, respectively.

Dark-field images were taken to analyze the amorphous and crystalline phases in detail (cf. Fig. 3; the objective aperture was placed at distance of 4.7 nm^{-1} from the transmitted beam to include a section of the strongest diffraction ring of the amorphous phase as well as, depending on their lattice orientation, reflections of B2 and B19′ nanograins). In the case of PS, Figure 3a shows an area of the amorphous bands. Nanograins that overlap in the TEM projection lead to strong variations in contrast. Frequently, narrow fringes with a spacing <5 nm are encountered caused by a moiré contrast effect [9]. Well-defined grain boundaries are not observed. It is important to note that the amorphous phase could not be identified either by dark-field images taken using different positions of the objective aperture or by bright-field images. However, SADPs containing strong diffuse rings unambiguously indicate the presence of a rather large volume fraction of amorphous phase. Therefore, it is concluded that in the case of PS the presence of the amorphous phase in TEM bright- and dark-field images is obscured by nanograins that overlap in the TEM projection.

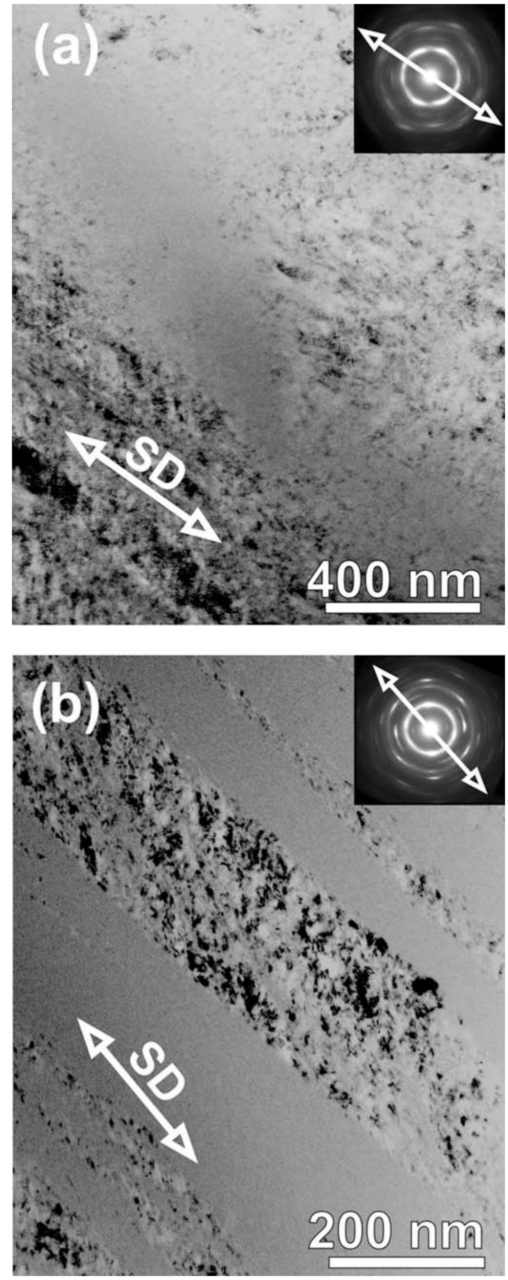

Figure 2. TEM bright-field images of HPT-deformed NiTi (the shear direction SD is indicated; corresponding SADPs are shown as insets). (a) PS. Embedded in a nanocrystalline phase, an amorphous band runs along SD. Due to an overlap of the crystalline and amorphous phases, the boundaries of the band appear to be curved and rather diffuse. (b) RS. Amorphous ribbons show well-defined and straight interfaces with respect to the nanocrystalline phase.

In the case of RS, Figure 3b shows clearly distinguishable nanocrystalline and amorphous phases; most of the nanograins show dark contrast with respect to the band-shaped amorphous structures (considering the texture, the position of the objective aperture was selected to include the strong amorphous ring and to exclude most of the lattice reflections). An elongated morphology of the nanograins is frequently observed (long direction inclined up to 40° with respect to the SD). Compared to the PS, moiré fringes are significantly less frequent, indicating that in the case of the RS most of the grain